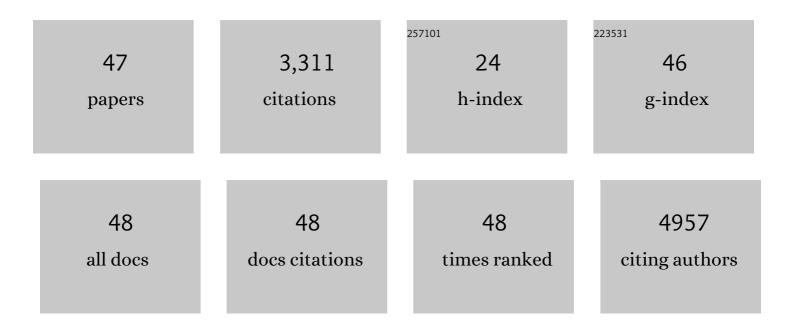
Eric Schaible

List of Publications by Year in descending order

Source: https://exaly.com/author-pdf/653988/publications.pdf Version: 2024-02-01



FDIC SCHAIRIE

#	Article	IF	CITATIONS
1	Liquid-free covalent reinforcement of carbon nanotube dry-spun yarns and free-standing sheets. Carbon, 2022, 187, 415-424.	5.4	11
2	Distinguishing Gas-Phase and Nanoparticle Contributions to Small-Angle X-ray Scattering in Reacting Aerosol Flows. Journal of Physical Chemistry A, 2022, 126, 3015-3026.	1.1	6
3	Soot-particle core-shell and fractal structures from small-angle X-ray scattering measurements in a flame. Carbon, 2022, 196, 440-456.	5.4	10
4	Nanolattice-Forming Hybrid Collagens in Protective Shark Egg Cases. Biomacromolecules, 2022, 23, 2878-2890.	2.6	0
5	Mechanically tunable elastomer and cellulose nanocrystal composites as scaffolds for <i>in vitro</i> cell studies. Materials Advances, 2021, 2, 464-476.	2.6	15
6	Effect of crystallization of the polyhedral oligomeric silsesquioxane block on self-assembly in hybrid organic-inorganic block copolymers with salt. Giant, 2021, 6, 100055.	2.5	10
7	Nanolatticed Architecture Mitigates Damage in Shark Egg Cases. Nano Letters, 2021, 21, 8080-8085.	4.5	2
8	High-yield growth kinetics and spatial mapping of single-walled carbon nanotube forests at wafer scale. Carbon, 2020, 159, 236-246.	5.4	15
9	The role of collagen in the dermal armor of the boxfish. Journal of Materials Research and Technology, 2020, 9, 13825-13841.	2.6	7
10	Structure and Mechanical Adaptability of a Modern Elasmoid Fish Scale from the Common Carp. Matter, 2020, 3, 842-863.	5.0	47
11	Dynamic Structure and Phase Behavior of a Block Copolymer Electrolyte under dc Polarization. ACS Applied Materials & Interfaces, 2020, 12, 57421-57430.	4.0	13
12	Electrophoresis Assisted Printing: A Method To Control the Morphology in Organic Thin Films. ACS Applied Materials & Interfaces, 2020, 12, 5219-5225.	4.0	6
13	Biomimetics: On the Origins of Fracture Toughness in Advanced Teleosts: How the Swordfish Sword's Bone Structure and Composition Allow for Slashing under Water to Kill or Stun Prey (Adv. Sci.) Tj ETQq1 1 0.784	¦31s4orgBT	/O¥erlock 1(
14	Chronic kidney disease and aging differentially diminish bone material and microarchitecture in C57Bl/6 mice. Bone, 2019, 127, 91-103.	1.4	37
15	On the Origins of Fracture Toughness in Advanced Teleosts: How the Swordfish Sword's Bone Structure and Composition Allow for Slashing under Water to Kill or Stun Prey. Advanced Science, 2019, 6, 1900287.	5.6	14
16	Mechanical Competence and Bone Quality Develop During Skeletal Growth. Journal of Bone and Mineral Research, 2019, 34, 1461-1472.	3.1	41
17	Correlations between Salt-Induced Crystallization, Morphology, Segmental Dynamics, and Conductivity in Amorphous Block Copolymer Electrolytes. Macromolecules, 2018, 51, 1733-1740.	2.2	27
18	Contributions of Material Properties and Structure to Increased Bone Fragility for a Given Bone Mass in the UCD-T2DM Rat Model of Type 2 Diabetes. Journal of Bone and Mineral Research, 2018, 33, 1066-1075.	3.1	57

ERIC SCHAIBLE

#	Article	IF	CITATIONS
19	Modulation of Carrier Type in Nanocrystal-in-Matrix Composites by Interfacial Doping. Chemistry of Materials, 2018, 30, 2544-2549.	3.2	1
20	Novel Defense Mechanisms in the Armor of the Scales of the "Living Fossil―Coelacanth Fish. Advanced Functional Materials, 2018, 28, 1804237.	7.8	61
21	In Situ X-ray Scattering Studies of the Influence of an Additive on the Formation of a Low-Bandgap Bulk Heterojunction. Chemistry of Materials, 2017, 29, 2283-2293.	3.2	23
22	In situ dynamic observations of perovskite crystallisation and microstructure evolution intermediated from [PbI6]4â^' cage nanoparticles. Nature Communications, 2017, 8, 15688.	5.8	191
23	Effect of block copolymer morphology on crystallization and water transport. Polymer, 2017, 120, 209-216.	1.8	10
24	Printing Fabrication of Bulk Heterojunction Solar Cells and In Situ Morphology Characterization. Journal of Visualized Experiments, 2017, , .	0.2	1
25	Note: Setup for chemical atmospheric control during <i>in situ</i> grazing incidence X-ray scattering of printed thin films. Review of Scientific Instruments, 2017, 88, 066101.	0.6	13
26	An <i>in situ</i> GISAXS study of selective solvent vapor annealing in thin block copolymer films: Symmetry breaking of inâ€plane sphere order upon deswelling. Journal of Polymer Science, Part B: Polymer Physics, 2016, 54, 331-338.	2.4	40
27	Intrinsic mechanical behavior of femoral cortical bone in young, osteoporotic and bisphosphonate-treated individuals in low- and high energy fracture conditions. Scientific Reports, 2016, 6, 21072.	1.6	65
28	Thermal stability and thermal aging of poly(vinyl chloride)/MgAl layered double hydroxides composites. Chinese Journal of Polymer Science (English Edition), 2016, 34, 542-551.	2.0	21
29	Real-time X-ray scattering studies of film evolution in high performing small-molecule–fullerene organic solar cells. Journal of Materials Chemistry A, 2015, 3, 8764-8771.	5.2	42
30	Ordering in Polymer Micelle-Directed Assemblies of Colloidal Nanocrystals. Nano Letters, 2015, 15, 8240-8244.	4.5	21
31	Topological Effects on Globular Proteinâ€ELP Fusion Block Copolymer Selfâ€Assembly. Advanced Functional Materials, 2015, 25, 729-738.	7.8	40
32	On the tear resistance of skin. Nature Communications, 2015, 6, 6649.	5.8	297
33	Nanocrystal Superlattice Embedded within an Inorganic Semiconducting Matrix by in Situ Ligand Exchange: Fabrication and Morphology. Chemistry of Materials, 2015, 27, 2755-2758.	3.2	10
34	Alendronate treatment alters bone tissues at multiple structural levels in healthy canine cortical bone. Bone, 2015, 81, 352-363.	1.4	58
35	Fast Printing and In Situ Morphology Observation of Organic Photovoltaics Using Slotâ€Die Coating. Advanced Materials, 2015, 27, 886-891.	11.1	117
36	In Situ Morphology Studies of the Mechanism for Solution Additive Effects on the Formation of Bulk Heterojunction Films. Advanced Energy Materials, 2015, 5, 1400975.	10.2	102

ERIC SCHAIBLE

#	Article	IF	CITATIONS
37	Fracture resistance of human cortical bone across multiple length-scales at physiological strain rates. Biomaterials, 2014, 35, 5472-5481.	5.7	125
38	Protective role of Arapaima gigas fish scales: Structure and mechanical behavior. Acta Biomaterialia, 2014, 10, 3599-3614.	4.1	161
39	Effect of sequential treatments with alendronate, parathyroid hormone (1–34) and raloxifene on cortical bone mass and strength in ovariectomized rats. Bone, 2014, 67, 257-268.	1.4	24
40	Mechanical adaptability of the Bouligand-type structure in natural dermal armour. Nature Communications, 2013, 4, 2634.	5.8	277
41	Evolution of Ordered Metal Chalcogenide Architectures through Chemical Transformations. Journal of the American Chemical Society, 2013, 135, 7446-7449.	6.6	30
42	Morphology and Optical Properties of P3HT:MEH-CN-PPV Blend Films. Macromolecules, 2013, 46, 4491-4501.	2.2	47
43	Noninvasive histological comparison of bone growth patterns among fossil and extant neonatal elephantids using synchrotron radiation X-ray microtomography. Journal of Vertebrate Paleontology, 2012, 32, 939-955.	0.4	27
44	Characterization of the effects of x-ray irradiation on the hierarchical structure and mechanical properties of human cortical bone. Biomaterials, 2011, 32, 8892-8904.	5.7	250
45	Age-related changes in the plasticity and toughness of human cortical bone at multiple length scales. Proceedings of the National Academy of Sciences of the United States of America, 2011, 108, 14416-14421.	3.3	325
46	A SAXS/WAXS/GISAXS Beamline with Multilayer Monochromator. Journal of Physics: Conference Series, 2010, 247, 012007.	0.3	522
47	Characterizing the nano and micro structure of concrete to improve its durability. Cement and Concrete Composites, 2009, 31, 577-584.	4.6	91